

Video Article

Diffuse Optical Spectroscopy for the Quantitative Assessment of Acute Ionizing Radiation Induced Skin Toxicity Using a Mouse Model

Lee Chin^{1,2}, Elina Korpela³, Anthony Kim¹, Darren Yohan², Carolyn Niu⁴, Brian C. Wilson³, Stanley K. Liu^{1,3}¹Department of Radiation Oncology, University of Toronto²Department of Physics, Ryerson University³Department of Medical Biophysics, University of Toronto⁴Ontario Cancer Institute / Campbell Family Institute for Cancer ResearchCorrespondence to: Lee Chin at lee.chin@sunnybrook.caURL: <https://www.jove.com/video/53573>DOI: [doi:10.3791/53573](https://doi.org/10.3791/53573)

Keywords: Medicine, Issue 111, Diffuse optical spectroscopy, biomarkers, microvasculature, nude mouse, hemoglobin, oxygen saturation, ionizing radiation

Date Published: 5/27/2016

Citation: Chin, L., Korpela, E., Kim, A., Yohan, D., Niu, C., Wilson, B.C., Liu, S.K. Diffuse Optical Spectroscopy for the Quantitative Assessment of Acute Ionizing Radiation Induced Skin Toxicity Using a Mouse Model. *J. Vis. Exp.* (111), e53573, doi:10.3791/53573 (2016).

Abstract

Acute skin toxicities from ionizing radiation (IR) are a common side effect from therapeutic courses of external beam radiation therapy (RT) and negatively impact patient quality of life and long term survival. Advances in the understanding of the biological pathways associated with normal tissue toxicities have allowed for the development of interventional drugs, however, current response studies are limited by a lack of quantitative metrics for assessing the severity of skin reactions. Here we present a diffuse optical spectroscopic (DOS) approach that provides quantitative optical biomarkers of skin response to radiation. We describe the instrumentation design of the DOS system as well as the inversion algorithm for extracting the optical parameters. Finally, to demonstrate clinical utility, we present representative data from a pre-clinical mouse model of radiation induced erythema and compare the results with a commonly employed visual scoring. The described DOS method offers an objective, high through-put evaluation of skin toxicity via functional response that is translatable to the clinical setting.

Video Link

The video component of this article can be found at <https://www.jove.com/video/53573/>

Introduction

Technological improvements in radiation therapy (RT) planning and delivery now allow for highly conformal therapeutic doses to be delivered to the tumor region, while simultaneously sparing normal surrounding structures. Yet, acute and sometimes severe toxicities are unavoidable when the high dose target is in close proximity to the skin. If severe enough, the resulting normal tissue damage can negatively affect the RT treatment outcome and patient quality of life^{1,2}.

Despite the detrimental consequences, present management of radiation skin erythema remains nonspecific, employing creams or ointments that ignore the underlying biological mechanisms leading to damage. These approaches are based upon minimizing symptoms rather than the cause. Moreover, the timing and administration of interventional therapies is complicated by the qualitative and subjective nature of radiation skin injury assessment. While several recognized organizations (RTOG, EORTC) provide visual grading recommendations, institutions vary in their choice of preferred scoring, thereby obscuring comparisons of normal tissue toxicities for the purposes of meta-analyses. Further, such grading systems are crude and prone to inter-observer variability, such that differences in radiation injury severity may be indiscernible in studies evaluating toxicity reduction strategies.

Rather than visually describing the degree of erythema in irradiated skin, an alternative approach is to measure parameters that quantitatively describe the underlying physiological changes that occur in the organ. Blood hemoglobin (Hb), tissue oxygen saturation (StO₂) or oxygenated hemoglobin (oxyHb) levels have been used as proxies for irradiation-induced erythema in mice³⁻⁶. Following irradiation, total Hb levels undergo fluctuations, but oxyHb or StO₂ undergo a characteristic early sharp rise, followed by a fall and another more persistent rise^{3,6}. When irritants are used to induce skin erythema, vascular oxyHb levels directly correlate with the severity of the local erythema and inflammation⁷.

Diffuse optical spectroscopy (DOS) employs near-infrared light to provide functional information on the biochemical and microstructural components of vital tissues components. This quantitative, non-invasive optical technology offers a method to measure the cytokine-induced vasodilation in blood vessels that occur during erythema via functional surrogates of Hb concentration and StO₂. Recent studies comparing DOS measured parameters with controlled clinical scoring methods⁸⁻¹¹ indicate the potential of the technique for overcoming the limitations inherent to current grading systems.

Here we describe an in-house, portable, DOS system that employs functional surrogates for quantitatively detecting differences in radiation-induced skin toxicity in a pre-clinical mouse model⁵. The described platform may provide a means of standardized erythema scoring with

high sensitivity for early detection and subtle differentiation of interventional drug response. Moreover, with only minor adaptations, the instrumentation may eventually be employed clinically for real-time bedside monitoring.

Protocol

The following methods are in accordance with the guidelines of the Sunnybrook Research Institute Animal Care Ethics Committee.

1. Diffuse Reflectance Spectroscopy System

1. Collect diffuse reflectance spectra using a handheld, fiber-optic probe and portable spectroscopic acquisition system that has been previously described (Kim *et al.* 2010) and is briefly reviewed in **Figure 1** (and related captions) for completeness^{1,2}.

2. Preparation of Mouse Model of Acute Radiation Skin Damage

1. Order 6-week old mice (preferably hairless, such as athymic or SKH-1) and allow them to acclimate in the animal facility for a week before starting experiments. Reserve at least 3 mice for a non-irradiated control group and 5 mice for an irradiated group.
2. Before baseline DOS measurements and irradiation, label the mice using ear punches or permanent marker markings on the tail. If mice are not nude, remove the hair on a 2 cm by 2 cm patch of flank skin, but this may cause skin irritation.

3. Diffuse Optical Spectroscopy Data Acquisition

1. Turn on the power supply to the electronics.
2. For mouse skin, set the signal parameters for the acquisition software by typing in 25 msec for collection time, 25 for signal averages and 1 for boxcar filter width. These parameters offer a reasonable balance between acquisition time and signal to noise.
3. Using custom programmed acquisition software, automatically acquire a background reading, R_{bg} (LED off) and diffuse reflectance at two source-detector separation distances, R_{meas} (260 μm , 520 μm) by clicking the "Acquire" button. The total acquisition time is ~ 2 sec.
4. Switch off all fluorescent room lights by pressing on the room light switch before performing measurements.
NOTE: Fluorescent room light interfere with the detected signal (these lights produce a time-varying light intensity and thus it is difficult to subtract as a background signal). Although incandescent bulbs may be employed keep the lights at a distance from the DOS probe to avoid high background levels (and poor signal to noise).

4. Animal Anesthesia and Baseline DOS Measurements

1. Prepare the anesthesia machine by ensuring that all connections are intact and liquid isoflurane level is adequate. Use an anesthesia induction chamber with an attached tube and nose cone that can be taped down to a sterilized, softly padded surface within comfortable reach of the DOS probe.
2. Anaesthetize one cage of mice at a time in the induction chamber by inducing with 4% isoflurane for 30 sec. Lower the isoflurane amount to 2% for the next 2 min. Verify that the mouse is anaesthetized by observing no response from pinching a toe of the hind limb.
3. Quickly move one mouse onto the sterilized DOS probing area, place it on its side, fasten its snout into the nose cone and open the nose cone tubing to the flow of anesthesia (2% isoflurane).
NOTE: If the procedure takes longer than 1 - 2 min, apply vet ointment on the eyes to prevent dryness.
4. Before acquiring mouse skin measurements, sterilize the probe by wiping with 70% ethanol. Do not sterilize the skin.
5. Place the probe gently on the flank skin making sure to avoid dispersing the local vasculature. Hold the probe by hand for the duration of the measurement.
6. Acquire reflectance data by probing a flank skin area of about 2 cm by 2 cm (the area to be irradiated) by following the 5-dot formation on a die. Keep this probing pattern, area, probe pressure and body side (left or right) consistent for all subsequent measurements.
NOTE: The complete scan takes approximately 60 sec. Probe pressure should be just enough to obtain a scan without dispersing local vasculature.
7. Move the mouse into a recovery cage, and move the next mouse over to the DOS probing area. Repeat steps 4.2 - 4.6 until all mice have been measured. Do not leave an animal unattended until it has regained sufficient consciousness to maintain sternal recumbency.

5. Animal irradiation

NOTE: This protocol requires the use of an irradiator, and animal preparation may need to be adjusted to meet the needs of the irradiator device. During irradiation, only the small area of flank skin should be exposed to the radiation beam. The irradiator should be located in a sterile facility and appropriate cage sterilization should be observed when returning mice to their sterile housing area.

1. Prepare the anesthesia machine (as in steps 4.1 - 4.2) and anaesthetize one mouse at a time in the induction chamber before preparing it for irradiation.
2. Remove the mouse from the induction chamber, gently pinch the flank skin and place tape over and below the stretched skin, forming a flap.
3. Place the mouse onto a plexiglass stage and cover the body with a custom lead jig (a working design is a rectangular box with the bottom and at least one end open, along with a side window to allow flank skin to be pulled through). Pull the skin flap through the jig window and gently tape the flap onto the stage.
NOTE: The custom lead jig is small enough to immobilize the mouse. If the custom jig does not completely immobilize the mouse, then use additional restrainers and/or administer ketamine (80 - 100 mg/kg) and xylazine (10 - 12.5 mg/kg) via intraperitoneal injection to keep the mouse immobilized throughout the entire irradiation procedure.

- Place the plexiglass stage with the jig and mouse into the irradiator. Determine the settings (skin distance from x-ray source, voltage, duration and amperage) and deliver the desired dose (e.g., 11 cm from a 160 kVp x-ray source for 2.5 min with 6.3 mA).
NOTE: Use CAUTION with the x-ray source by following machine use guidelines to avoid burns and DNA damage.
NOTE: Athymic nude mice develop moist desquamation around 14 days post irradiation in response to 35 Gy, but only minor patchy desquamation with 17 Gy.
- Take the apparatus and mouse out of the irradiator, remove the shielding, remove the tape and place it into an individual recovery cage. Return the mouse to its normal shared cage after it has recovered from the anesthesia. Repeat steps 5.2 - 5.4 for all mice, and perform a sham operation on control mice.
- After irradiation, house the animals in their regular conditions. If abnormal behavior develops (e.g., hunched posture, which may signify pain), consult a veterinarian to diagnose the problem. Pain alleviation may include administering 0.1 mg/kg buprenorphine subcutaneously or as directed by the veterinarian. If weight loss exceeds 20% of normal body mass, house it separately in its own cage and provide high-nutrient food.

6. Follow-up DOS Measurements

- Monitor and measure skin reaction intensity using the quantitative DOS technique. Visual inspection of skin changes and previous work suggest that large changes in DOS parameters can be expected (relative to baseline) around 6 - 12 days following irradiation^{3,4}. However, since appreciable changes may take place even earlier or later depending on the model, other measurement time points may be useful to investigate.
- Set up DOS equipment and calibrations as described in section 3. Prepare the anesthesia machine and acquire DOS measurements as described in section 4.

7. Post-acquisition Processing

NOTE: All steps in the following section are performed using a custom program created in a high performance software environment. Standardized naming conventions for each spectral acquisition file are employed to allow for batch processing. All steps are illustrated in **Figure 2**.

- Subtract the baseline (noise floor) from all the measured spectra including the background reading.
- Subtract the background reading, R_{bg} (LED off), obtained in Step 3.3 from the measurement spectrum, R_{meas} .
NOTE: For the remainder of this article all spectra are assumed to be noise floor and background subtracted and referred to as R_{corr} .
- Convert R_{corr} to absolute reflectance, R_{abs} , as described in references 1,2 in Section 1.
 - Obtain relative reflectance measurements, R_{rel} , in Intralipid-20% phantoms (Fresenius Kabi, Sweden) phantoms with increasing 3% aliquot fractions up to 48% (i.e., 3%, 6%, 9%, ..., 48%) and create of plot of R_{rel} versus Intralipid concentration.
 - Generate an absolute plot of R_{abs} versus μ_s' using the diffusion equation for reflectance.¹⁴
 - Match the peak of both curves and adjust the R_{rel} x-axis to match the R_{abs} x-axis.
 - At a given wavelength and source-detector separation, scale the y-axis using:

$$Scale(L, r) = \frac{\langle R_{rel}(us' \text{EV}) \rangle}{\langle R_{meas}(us' \text{EV}) \rangle}$$

NOTE: In the following section, all fitting of measurements will refer to R_{abs} .

8. Spectral Data Fitting

NOTE: The following section outlines the theory and fitting algorithm utilized for extracting functional parameters of mice skin. For all theory employed, refer to the following articles¹⁴⁻¹⁸ and references therein. All equations are assumed to be programmed in a high end scientific software environment (containing pre-programmed modules) commonly used in physics or engineering labs.

- Program a function that describes the absorption spectrum, $\mu_a(\lambda)$ of skin as the sum of relevant individual chromophores in the spectral range of interest using the equation:

$$\mu_a(\lambda) = H_b [StO_2 \mu_a^{oxyHb}(\lambda) + (1 - StO_2) \mu_a^{deoxyHb}(\lambda)]$$
 Here, H_b is the total hemoglobin concentration (g/L), while StO_2 is the unitless oxygen saturation ranging from 0 to 1.
- Obtain oxy, $\mu_a^{oxyHb}(\lambda)$, and deoxy, $\mu_a^{deoxyHb}(\lambda)$, hemoglobin spectra (stored as text files) from the on-line collection of Prahl¹⁹.
- Program a function that describes the scattering spectrum of skin, $\mu_s'(\lambda) = A \left(\frac{\lambda}{\lambda_0}\right)^{-k}$, using a power law dependence, where A (cm^{-1}) is the value of μ_s' at $\lambda_0 = 1$ nm and k is a medium dependent power factor¹⁶.
- Program a mathematical function for the forward model of diffuse reflectance based on equations from reference 14 that incorporate the spectral equations from Steps 8.2 - 8.3 into the forward model function (i.e., $R(r, \mu_a(\lambda), \mu_s'(\lambda)) = R(r, H_b, StO_2, A, k)$).
NOTE: While various models exist, the steady-state diffusion theory equation provides a simple and accurate description of the light distribution in tissue.
- Program a function that squares the difference between the forward modeled reflectance spectra from Section 8.4 and the measured reflectance spectra.
- Iteratively change H_b , StO_2 , A , and k until the least squares difference function in Section 8.5 is smallest. MatLab's `lsqcurvefit` can be used to automatically perform this step.
- Repeat steps 8.5 - 8.6 to obtain DOS parameters (H_b , StO_2 , A , and k) for all measured reflectance data sets.

8. Plot the relative change in DOS parameter with the corresponding unique baseline measurement using the average of each mouse's set of 3 - 5 normalized probe spot measurements. These plots are created using MatLab's plot command.

9. Visual Radiation Dermatitis Scoring Period

1. Monitor and score skin reaction intensity using a qualitative grading scale (see Douglas and Fowler grading scale²⁰) after irradiation every 48 hr (one may also observe changes 3 - 24 hr following irradiation). Two blinded investigators are ideal. Acquiring photographs with a hand-held camera and reference scale (*i.e.*, ruler) may help with evaluations.
2. NOTE: Scoring the skin every two days after irradiation may help determine optimal DOS measurement times for the model. More frequent scoring may yield important data depending on the model and research question.
3. Plot the median of each group at each time point. Compare groups at specific time points or the median overall areas under each curve.
4. After mice have been followed to the point of skin healing that is desired (*e.g.*, 4 weeks), euthanize the mice by an appropriate (approved) method.

Representative Results

The DOS reflectance technique provides an objective alternative to traditional qualitative methods of evaluating radiation induced skin toxicity. Visual changes in skin appearance following toxic doses of radiation present as alterations in both the magnitude and shape of the measured reflectance spectra. Both are related to functional changes in the underlying cellular microstructure and physiological tissue state. In this section, representative results from previously published work by Yohan *et al.* 2014⁹ are reviewed.

Figure 3 (left) show representative spectra (thin blue lines) measured at a 260 μm source-separation in an athymic mouse model of skin erythema 6 days after 40 Gy irradiation. Compared to pre-irradiation (**Figure 3**, right panel), differences in the spectral shape at $\sim 550\text{-}650$ nm are observed, likely due to an increase in oxygenated hemoglobin. A small rise in absolute reflectance is also seen that is correlated to an increase in tissue scattering power. The observed spectra on day 6 following irradiation correlated to a visual skin score of 0.75.

An evaluation of post irradiation reflectance changes at select wavelengths does not make use of the complete reflectance spectrum and also carries the potential issue of noise sensitivity. However, fitting the complete spectrum allows the entire data set to be converted into intuitive optical biomarkers (H_b , StO_2). **Figure 3** show the resulting fits (solid green line) of the measured data (thin noisy line) using the equations presented in Section 4. Excellent agreement is observed, confirming that the choice of basis chromophores and scattering shape adequately describe the mouse skin model.

Due to the non-invasive and self-calibrating nature of the DOS system, measurements can be conveniently performed over multiple days in different lighting conditions. **Figure 4** shows relative changes in skin StO_2 for various time-points (6, 9, 12 days) in an irradiated mouse cohort ($n=8$) while **Figure 5** shows the corresponding qualitative skin reaction scores. A progressive increase in StO_2 is observed that is statistically different compared to pre-irradiation values over all 3 days ($p < 0.05$). These trends mirror the visually observed increases in skin damage severity that peak at day 12 (average score of ~ 3) demonstrating the potential of StO_2 as a visual scoring surrogate (**Figure 5**).

It should be noted that no statistically significant changes were seen for any of the returned optical biomarkers for the non-irradiated control group ($n=3$) over the 12 days measured (data not shown). Changes in A and k can also be monitored over time (**Figure 6**), and these indicate that the scattering properties of the skin are changing in response to the radiation.

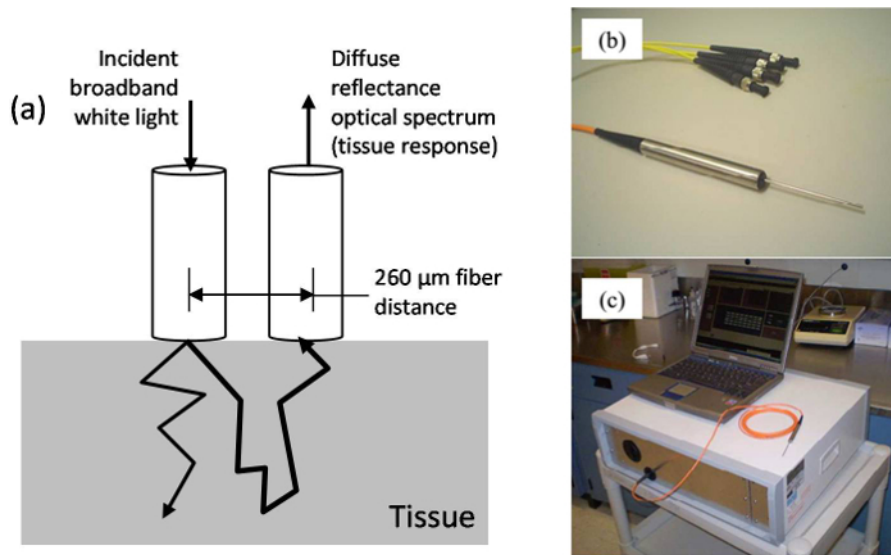


Figure 1. DOS instrumentation. (A) Schematic of the diffuse reflectance measurement geometry. (B) Fiber-optic probe: The optical probe consists of a linear array of 200 μm core optical fibers that are bundled into an 18 G metal needle and spaced 260 μm apart. Two source fibers are coupled to two broadband light emitting diodes while a detection fiber is connected to an optical spectrometer. By sequentially turning on each of the sources, the spectrometer can collect diffuse reflectance at distances of 260 μm and 520 μm from each of the source fibers. (C) Complete DOS system including laptop, attached fiber-optic probe and optic box: An automated data acquisition program is used to drive the sequential collection of spectra. The electronics are housed in an acquisition box that connects to the fiber-optic probe via SMA connectors. [Please click here to view a larger version of this figure.](#)

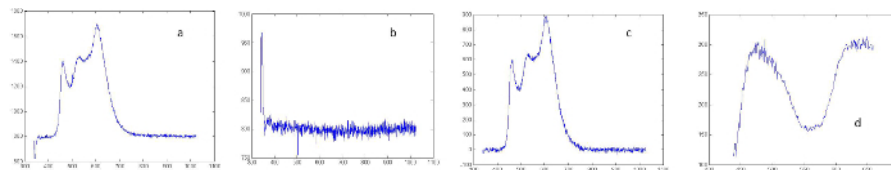


Figure 2. Spectral processing. All x-axis scales are in nm: (A) Raw relative spectra, the baseline is the reading approximately between 900 - 1,000 nm and approximately equal to the background signal. (B) Relative background reading. (C) Background and baseline subtracted relative spectra. (D) Absolutely calibrated spectrum following scaling of processed spectra shown in (C). [Please click here to view a larger version of this figure.](#)

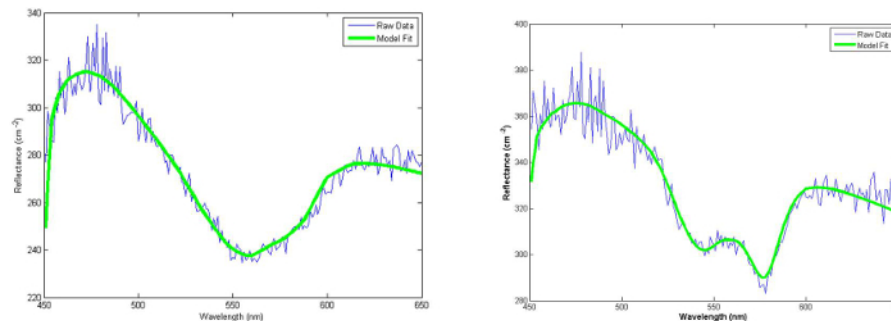


Figure 3. Typical white light reflectance spectra of non-irradiated (left) and irradiated (right) mouse skin 6 days post irradiation. Excellent agreement between measurement (noisy blue) and fits (solid green) were typically observed. Two key differences were seen between the two groups: 1) an overall increase in absolute reflectance and 2) a distinct change in spectral shape between 550 - 600 nm. With permission from Yohan *et al.* 2014⁵. [Please click here to view a larger version of this figure.](#)

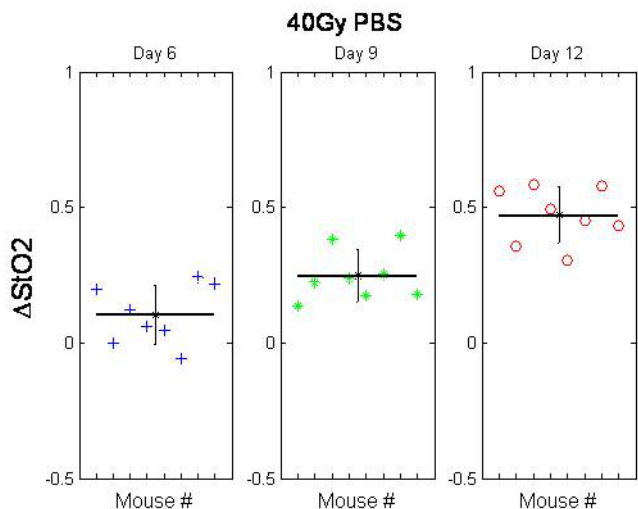


Figure 4. Change in the oxygenation fraction of mouse skin following 40 Gy irradiation. The baseline-normalized mean difference between the two groups (per mouse) is significant for Days 6 (Box 1), 9 (Box 2) and 12 (Box 3). With permission from Yohan *et al.* 2014⁵. [Please click here to view a larger version of this figure.](#)

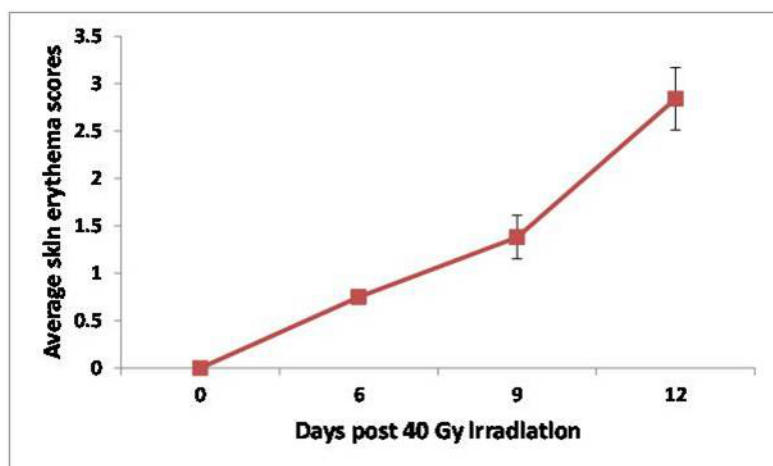


Figure 5. Average qualitative skin reactions scores (n=8) as a function of days following 40 Gy irradiated mice skin. Adapted from Yohan *et al.* 2014⁵. [Please click here to view a larger version of this figure.](#)

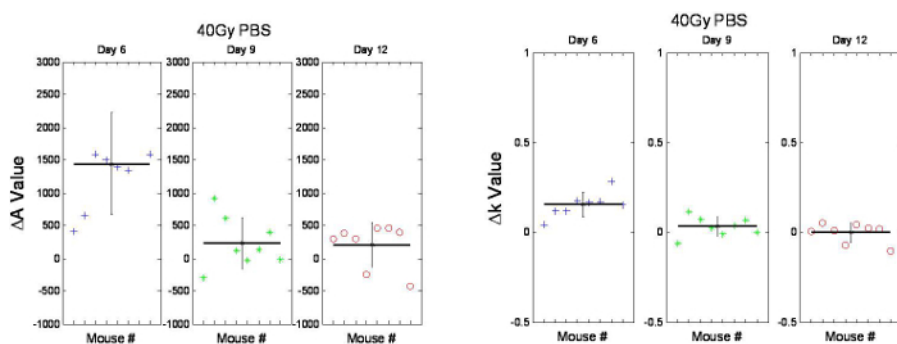


Figure 6. Relative changes in A and k of mouse skin following 40 Gy irradiation on Days 6 (Box 1), 9 (Box 2) and 12 (Box 3). The change in A (left side) and k (right side) on Day 6 (Box 1, left and right sides) was found to be significant ($p < 0.026$). With permission from Yohan *et al.* 2014⁵. [Please click here to view a larger version of this figure.](#)

Discussion

A DOS approach for quantitatively assessing radiation skin toxicities using optical biomarkers has been presented. Visual skin toxicity scoring systems require expert training and even then are prone to inter-observer variability and subjectivity. The DOS system and analysis software is simple to use, requires minimal training and returns objective functional parameters for interpreting physiological changes in skin. Furthermore, instead of describing the appearance of a skin lesion as a single parameter, DOS provides a wealth of information in spectral

shape, optical properties and functional / microstructural parameters that offer an added degree of sensitivity and specificity not available in current qualitative scoring methods. Sections 1 and 7 highlight the main processing steps for obtaining absolute spectral data that can be utilized for quantitative fitting of optical biomarkers. Background and baseline subtraction are vital to allow the user to perform the DOS measurements under normal lighting conditions. Section 8 provides the necessary models and equations needed to describe athymic mice before and after x-ray irradiation. Here, the choice of appropriate absorbers is vital for an accurate description of the measured spectra. It is advised that the user thoroughly investigate in the literature the key absorbers that dominate the wavelength range and tissue of interest used in a given study prior to constructing an optical biomarker fitting model. Finally, Sections 3-5 describe the handling of the athymic mice during DOS acquisition. To avoid disrupting the local vasculature, use gentle force to place the DOS probe on the mouse skin surface.

While relatively inexpensive compared to hyperspectral camera systems^{3,4}, a clear limitation of the described DOS approach is the use of a point probe for measuring diffuse reflectance. This reflectance geometry necessitates gentle contact with the skin and has the potential to introduce measurement uncertainty by dispersing the vasculature if consistent probe-skin pressure is not employed. Future designs of the DOS probe may incorporate a pressure sensor to maintain consistent results. Further, while the use of close source-detector separation (< 2-3 mm) allows for optical probing depths specific to the skin surface, the improved specificity comes at a loss of spatial resolution compared to 2D hyperspectral imaging. To minimize this limitation, a 5 point quadrant scan that captures the overall irradiated volume was employed. Despite the lack of spatial resolution, previous work in mice⁵ has shown the ability of optical biomarkers averaged over a sparse area to differentiate not only irradiated and non-irradiated skin but also the impact of skin sparing interventional drugs such as Vasculotide⁶.

It should be noted that while the overall system design can be modified for different skin models, the underlying basis spectra and scattering shape may need to be optimized. Specifically, while oxy- and deoxy-Hb well describe an athymic mouse model, the application of the same model to darker skin may require the addition of melanin for optimal fitting. In addition, extension of the DOS bandwidth to higher wavelengths > 950 nm would necessitate the addition of water, which dominates at higher wavelengths. Furthermore, animal models with different skin thicknesses may require a different source-detector separation to optimize depth sensitivity. Lastly, the hairless feature makes algorithms simpler. Although non-hairless models may be optimal for certain research questions, they will require hair removal before DOS measurements, and skin irritation from this process may affect results. For research where total immune function is crucial, an immunocompetent hairless mouse (e.g., SKH-1) may serve as a better model due to its euthymic nature.

Important considerations for DOS probe measurements are consistent RT and estimation of the irradiated area. Temperature fluctuations can affect tissue Hb and StO₂ levels. Measuring a group of 3 non-irradiated animals at each data collection time may serve as a baseline to which unintended environmental fluctuations in parameter values can be normalized. Additionally, the irradiated area may be difficult to estimate (if skin flap preparations were not consistent) before damage begins to manifest visually around day 5 (40 Gy). If using black permanent marker to dot the boundaries of the radiation-exposed skin, avoid excessive ink use to prevent ink smudging, which can compromise readings.

An added feature of the system is the ability to separate absorption from scattering properties. While alternative hyperspectral imaging systems also provide the ability to monitor oxyHb and Hb concentration, the free-space geometry of hyperspectral imaging is unable to resolve scattering changes. This limitation may result in inaccuracies in the returned oxyHb, Hb and StO₂ parameters if significant changes in scattering occur due to erythema (redness). Further, monitoring of scattering changes using DOS may provide additional optical biomarkers for erythema evaluation. As shown in **Figure 6**, the initial results from Yohan *et al.* (2014) indicate that A and k demonstrate a temporal trend following ionizing radiation that does not correlate with trends observed from other alternative methods such as visual scoring systems. This indicates that scattering changes do not manifest in a visually descriptive manner and may in fact be describing a separate biological process. Therefore, compared to alternative methods, DOS provides a high resolution for superficial scattering changes, an avenue for investigating novel skin damage biomarkers that may be separate from the usual Hb-based measurements.

Although our model employs a large single radiation dose (rather than multiple small fractionated doses that are used in the clinical setting), this mimics the pathophysiology of acute human skin radiotoxicity²¹. It is envisioned that with further optimization, DOS may provide a quantitative approach for automated and standardized scoring of radiation induced skin reactions. After mastering this technique, future applications may include monitoring differences between skin sparing therapeutics (e.g., comparing oxyHb levels between a control and experimental treatment for skin radioprotection, or for wound healing promotion). While ideal for high-throughput drug screening in animal models, the DOS system is potentially adaptable to the clinical environment due to ease of usability and the ability to measure in normal lighting conditions. In this case, the probe design may require minor modifications with slightly larger optode separations to account for the increased thickness of human skin. A clinical DOS system would allow for on-line evaluation of interventional therapies that could minimize painful skin reactions and improve patient comfort and compliance. In the future, it may be interesting to expand DOS-based quantification to the features of chronic radiation induced skin damage (e.g., fibrosis).

Disclosures

The authors have nothing to disclose.

Acknowledgements

This work was supported by research grants awarded to SKL from Abbott CARO (Canadian Association of Radiation Oncologists) Uro-Oncologic Radiation Awards and the Alan E. Tiffin Foundation. EK was supported by the Frederick Banting and Charles Best Canada Graduate Scholarship, the Scace Graduate Fellowship in Prostate Cancer Research and Paul Starita Graduate Student Fellowship.

References

1. Hall, E. J. and Giaccia, A. J. *Radiobiology for the Radiologist*. J.B. Lippincott Company, Philadelphia, (2011).
2. Ryan, J. L. Ionizing Radiation: The Good, the Bad, and the Ugly. *J Invest Dermatol*. **132**, 985-993 (2012).

3. Chin, M.S., *et al.* Hyperspectral imaging for early detection of oxygenation and perfusion changes in irradiated skin. *J Biomed Opt.* **17(2)**:02601013 (2012).
4. Chin, M.S., *et al.* Skin perfusion and oxygenation changes in radiation fibrosis. *Plast. Reconstr. Surg.* **131** (4) , 707-716 (2013).
5. Yohan, D. *et al.* Quantitative monitoring of radiation induced skin toxicities in nude mice using optical biomarkers measured from diffuse optical reflectance spectroscopy. *Biomed. Opt. Express.* **5** (5) , 1309-1320 (2014).
6. Korpela, E. *et al.* Vasculotide, an Angiopoietin-1 mimetic reduces acute skin ionizing radiation damage in a preclinical mouse model. *BMC Cancer* **14**, 614 (2014).
7. Stamatatos, G.N., & Kollias, N. *In vivo* documentation of cutaneous inflammation using spectral imaging. *J. Biomed. Opt.* **12** (5) , 051603 (2007).
8. Turesson, I., Nyman, J., Holmberg, E., Oden, A. Prognostic factors for acute and late skin reactions in radiotherapy patients. *Int. J. Radiat. Oncol. Biol. Phys.* **36**, 1065-1075 (1995).
9. Rizza, L., D'Agostino, A., Girlando, A., & Puglia, C. Evaluation of the effect of topical agents on radiation-induced skin disease by reflectance spectrophotometry. *J. Pharm. Pharmacol.* **62** (6) , 779-785 (2010).
10. Wells, M., *et al.* Does aqueous or sucralfate cream affect the severity of erythematous radiation skin reactions? A randomised controlled trial. *Radiother. Oncol.* **73** (2) , 153-162 (2004).
11. Denham, J.W., & Hauer-Jensen, M. The radiotherapeutic injury-a complex 'wound'. *Radiother. Oncol.* **63** (2) , 129-145 (2002).
12. Kim, A., Roy, M., Dadani, F., and Wilson, B. C. A fiberoptic reflectance probe with multiple source-collector separations to increase the dynamic range of derived tissue optical absorption and scattering coefficients. *Opt. Express.* **18**, 5580-5594 (2010).
13. Kim, A., Khurana, M., Moriyama, Y., and Wilson, B. C. Quantification of *in vivo* fluorescence decoupled from the effects of tissue optical properties using fiber-optic spectroscopy measurements. *J. Biomed. Opt.* **15**, 067006 (2010).
14. Farrell, T.J., Patterson, M.S., Wilson, B.C. A diffusion theory model of spatially resolved, steady-state diffuse reflectance for the noninvasive determination of tissue optical properties *in vivo*. *Med. Phys.* **19(4)**:879-88 (1992).
15. Finlay, J.C., Foster T.H. Hemoglobin oxygen saturations in phantoms and *in vivo* from measurements of steady-state diffuse reflectance at a single, short source-detector separation. *Med Phys.* **31(7)**, 1949-59 (2004).
16. Mourant, J.R., Fusilier, T., Boyer, J., Johnson, T.M., and Bigio I.J. Predictions and measurements of scattering and absorption over broad wavelength ranges in tissue phantoms. *Appl Opt.* **36**, 949-957 (1997).
17. Corlu, A., *et al.* Uniqueness and wavelength optimization in continuous-wave multispectral diffuse optical tomography. *Opt. Lett.* **28**, 2339-2341 (2003).
18. Chin, L., Lloyd, B., Whelan, W. M. and Vitkin, A. Interstitial point radiance spectroscopy of turbid media. *J App Physics.* **105**, 102025 (2009).
19. Prahl, S. *Tabulated Molar Extinction Coefficient for Hemoglobin in Water.* <http://omlc.org/spectra/hemoglobin/summary.html> (1998).
20. Douglas, B.G. and Fowler, J.F.. The effect of multiple small doses of X rays on skin reactions in the mouse and a basic interpretation. *Radiat. Res.* **178** (2) , AV125-AV138 (1976).
21. Williams, J.P. *et al.* Animal models for medical countermeasures to radiation exposure. *Radiat. Res.* **173** (4) , 557-578 (2010).